HHS Public Access

Author manuscript

Nature. Author manuscript; available in PMC 2014 June 11.

Published in final edited form as:

Nature. 2014 February 6; 506(7486): 52–57. doi:10.1038/nature12988.

In vivo Discovery of Immunotherapy Targets in the Tumor Microenvironment

Penghui Zhou[1,*], **Donald R. Shaffer**[1,*], **Diana A. Alvarez Arias**[1], **Yukoh Nakazaki**[1], **Wouter Pos**[1], **Alexis J. Torres**[2], **Viviana Cremasco**[1], **Stephanie K. Dougan**[3], **Glenn S. Cowley**[4], **Kutlu Elpek**[1], **Jennifer Brogdon**[5], **John Lamb**[6], **Shannon Turley**[1], **Hidde L. Ploegh**[1], **David E. Root**[4], **J. Christopher Love**[2], **Glenn Dranoff**[1], **Nir Hacohen**[2], **Harvey Cantor**[1], and **Kai W. Wucherpfennig**[1]

[1]Dana-Farber Cancer Institute, Boston, MA 02115

[2]David H. Koch Institute for Integrative Cancer Research, Massachusetts Institute of Technology, Cambridge, MA 02142

[3]Whitehead Institute, Massachusetts Institute of Technology, Cambridge, MA 02142

[4]Broad Institute of MIT and Harvard, Cambridge, MA 02142

[5]Novartis Institutes for Biomedical Research, Cambridge, MA 02139

[6]Genomics Institute of the Novartis Research Foundation, San Diego CA 92121

Abstract

Recent clinical trials showed that targeting of inhibitory receptors on T cells induces durable responses in a subset of cancer patients, despite advanced disease. However, the regulatory switches controlling T cell function in immunosuppressive tumors are not well understood. Here we show that such inhibitory mechanisms can be systematically discovered in the tumor microenvironment. We devised an *in vivo* pooled shRNA screen in which shRNAs targeting negative regulators became highly enriched in tumors by releasing a block on T cell proliferation upon tumor antigen recognition. Such shRNAs were identified by deep sequencing of the shRNA cassette from T cells infiltrating tumor or control tissues. One of the target genes was Ppp2r2d, a regulatory subunit of the PP2A phosphatase family: In tumors, Ppp2r2d knockdown inhibited T

Correspondence and requests for materials should be addressed to kai_wucherpfennig@dfci.harvard.edu.
*These authors contributed equally

Supplementary information is linked to the online version of the paper at www.nature.com/nature.

Author Contributions

K.W.W., P.Z., S.T., G.D. and H.C. contributed to the overall study design; K.W.W., P.Z. and D.S. designed experiments; P.Z., D.A.A.A. and H.C. developed procedure for lentiviral infection of T cells and optimized approaches for adoptive T cell therapy; P.Z., D.S. and D.A.A.A. performed shRNA screen; G.S.C., D.E.R. and N.H. provided pooled shRNA library and advice on shRNA screen; Y.N. and G.D. provided B16-Ova cell line and advice on tumor model; A.J.T. and J.C.L. performed nanowell analysis of cytokine production, V.C. and S.T. performed histological studies, W.P. performed protein quantification by mass spectrometry, S.K.D. and H.L.P. provided mouse models; J.B., K.E. and J.L. performed microarray analysis; K.W.W., P.Z. and D.S. wrote the paper.

Competing financial interests

K.W.W. and G.D. served as consultants to Novartis.

The access number for microarray data is GSE53388 in the Genomic Spatial Event (GSE) database.

cell apoptosis and enhanced T cell proliferation as well as cytokine production. Key regulators of immune function can thus be discovered in relevant tissue microenvironments.

Introduction

Recent work has shown that cytotoxic T cells play a central role in immune-mediated control of cancer[1–7]. T cells are able to specifically detect and eliminate cancer cells following T cell receptor (TCR) mediated recognition of tumor-derived peptides bound to MHC proteins[8]. A series of studies have convincingly demonstrated that the extent of tumor infiltration by cytotoxic T cells is a critical factor determining the natural progression of diverse types of cancers[1–4,9–11]. A landmark study showed that the type, density, and location of cytotoxic T cells within tumors enabled better prediction of patient survival than histopathological methods used for staging of cancers. Strong infiltration of both the tumor center and the invasive tumor margin by cytotoxic T cells (which express the CD8 surface marker) was shown to correlate with a favorable prognosis, regardless of the local extent of tumor invasion and spread to local lymph nodes. Conversely, weak *in situ* expansion of CD8 T cells correlated with a poor prognosis even in patients with minimal tumor invasion[1]. However, in the majority of patients this natural defense mechanism is severely blunted by immunosuppressive cell populations recruited to the tumor microenvironment, including regulatory T cells, immature myeloid cell populations and tumor-associated macrophages[4,12–14]. Highly complex interactions among a variety of different cell types – including tumor cells, immune cells and stromal cells – in the tumor microenvironment thus contribute to clinical outcome.

The critical role of T cells in immune-mediated control of cancers is further underscored by therapeutic benefit following administration of monoclonal antibodies targeting inhibitory receptors on T cells, CTLA-4 and PD-1 [15–18]. Clinical benefit is enhanced by co-administration of antibodies targeting CTLA-4 and PD-1[19,20]. Particularly exciting is the finding that such antibodies can induce durable responses in a subset of patients with advanced disease. However, many of the regulatory pathways in T cells that result in loss of function within immunosuppressive tumor microenvironments remain unknown.

Immune cells perform complex surveillance functions throughout the body and interact with many different types of cells in distinct tissue microenvironments. Therapeutic targets for modulating immune responses are typically identified *in vitro* and tested in animal models at a late stage of the process. We postulated that the complex interactions of immune cells within tissues - many of which do not occur *in vitro* - offer untapped opportunities for therapeutic intervention. Here we have addressed the challenge of how targets for immune modulation can be systematically discovered *in vivo*.

Design of *in vivo* discovery approach

Pooled short hairpin RNA (shRNA) libraries have been shown to be powerful discovery tools[21–23]. We reasoned that shRNAs capable of restoring CD8 T cell function can be systematically discovered *in vivo* by taking advantage of the extensive proliferative capacity of T cells following triggering of the TCR by a tumor-associated antigen. When introduced

into T cells, only a small subset of shRNAs from a pool will restore T cell proliferation, resulting in their enrichment within tumors. Over-representation of active shRNAs within a pool can be quantified by deep sequencing of the shRNA cassette from tumors and secondary lymphoid organs (Fig. 1a).

We chose B16 melanoma, an aggressive tumor that is difficult to treat[24]. Melanoma cells expressed the surrogate tumor antigen ovalbumin (Ova), which is recognized by CD8 T cells from OT-I T cell receptor transgenic mice[25,26]. Initial experiments showed that such a screen could also be performed with pmel-1 T cells that recognize gp100, an endogenous melanoma antigen[27], but the signal/noise ratio was lower for pmel-1 T cells due to smaller T cell populations in tumors. Naïve T cells are difficult to infect with lentiviral vectors, and we therefore pretreated T cells for two days with the homeostatic cytokines IL-7 and IL-15 prior to spin infection with shRNA pools in a lentiviral vector. Successful transduction was monitored by surface expression of the Thy1.1 reporter (Extended Data Fig. 1a). T cells were injected into B6 mice bearing day 14 B16-Ova tumors. Seven days later, T cells were purified from tumors and secondary lymphoid organs (spleen, tumor-draining and irrelevant lymph nodes) for isolation of genomic DNA, followed by PCR amplification of the shRNA cassette (Extended Data Fig. 1b). The representation of shRNAs was then quantified in different tissues by Illumina sequencing.

In vivo shRNA pool screens

Two large screens were performed, with the first focusing on genes over-expressed in dysfunctional T cells (T cell anergy or exhaustion; 255 genes, 1,275 shRNAs divided into two pools), and the second on kinases/phosphatases (1,307 genes, 6,535 shRNAs divided into seven pools) (Table 1a). In these primary screens, each gene was represented by ~5 shRNAs (it is common that only one or two of such shRNAs have sufficient activity in pooled screens). We observed multiple distinct *in vivo* phenotypes. For certain genes, shRNAs were over-represented in all tested tissues compared to the starting T cell population (e.g. SHP-1), indicative of enhanced proliferation independent of TCR recognition of a tumor antigen. For other genes, there was a selective loss of shRNAs within tumors (e.g. ZAP-70, a critical kinase in the T cell activation pathway). We focused our analysis on genes whose shRNAs showed substantial over-representation in tumor but not spleen, a secondary lymphoid organ. Substantial T cell accumulation in tumors was observed for a number of shRNAs, despite the immunosuppressive environment. For secondary screens, we created focused pools in which each candidate gene was represented by ~15 shRNAs. Primary data from this analysis are shown for three genes in Fig. 1b: LacZ (negative control), Cblb (an E3 ubiquitin ligase that induces T cell receptor internalization)[28] and Ppp2r2d (not previously studied in T cells). For both Ppp2r2d and Cblb, five shRNAs were substantially increased in tumors (red) compared to spleen, while no enrichment was observed for LacZ shRNAs. Overall, 43 genes met the following criteria: ≥4-fold enrichment for 3 or more shRNAs in tumors compared to spleen (Table 1a, Extended Data Fig. 1c,d). The set included gene products previously identified as inhibitors of T cell receptor signaling (including Cblb, Dgka, Dgkz, Ptpn2) as well as other well-known inhibitors of T cell function (e.g. Smad2, Socs1, Socs3, Egr2), validating our approach (Table 1b, Extended Data Table 1).[29–31]

Target validation

We next confirmed at a cellular level that these shRNAs induce T cell accumulation in tumors. OT-I T cells were infected with lentiviral vectors driving expression of a single shRNA and a reporter protein (Thy1.1 or one of four different fluorescent proteins), and after seven days the frequency of shRNA-transduced T cells was quantified in tumors, spleens and lymph nodes by flow cytometry. When the control LacZ shRNA was expressed in CD8 T cells, the frequency of shRNA-expressing CD8 T cells was lower in tumors compared to spleen (~2-fold). In contrast, experimental shRNAs induced accumulation of CD8 T cells in tumors but not the spleen (Fig. 2a, Extended Data Fig. 2a). T cell accumulation in tumors was >10-fold relative to spleen for seven of these genes. The strongest phenotype was observed with shRNAs targeting Ppp2r2d, a regulatory subunit of the family of PP2A phosphatases[32]. A Ppp2r2d shRNA not only induced accumulation of OT-I CD8 T cells, but also CD4 T cells (from TRP-1 TCR transgenic mice)[33], with T cell numbers in tumors being significantly higher when Ppp2r2d rather than LacZ shRNA was expressed (36.3-fold for CD8; 16.2-fold for CD4 T cells) (Fig. 2b). CD8 T cell accumulation correlated with the degree of Ppp2r2d knock-down, and two Ppp2r2d shRNAs with the highest *in vivo* activity induced the lowest levels of Ppp2r2d mRNA (Extended Data Fig. 2b). Ppp2r2d knockdown was also confirmed at the protein level using a quantitative mass spectrometry approach (Fig. 2e). Ppp2r2d shRNA activity was specific because the phenotype was reversed when a Ppp2r2d cDNA (with wild-type protein sequence, but mutated DNA sequence at the shRNA binding site) was co-introduced with the Ppp2r2d shRNA (Fig. 2c, Extended Data Fig. 3). Furthermore, OT-I CD8 T cells over-expressed Ppp2r2d in tumors compared to spleen (in the absence of any shRNA expression), suggesting that it is an intrinsic component of the signaling network inhibiting T cell function in tumors (Fig. 2d). Microarray analysis of tumor-infiltrating T cells expressing different shRNAs showed that each shRNA induced a largely distinct set of gene expression changes, indicating that improved T cell function in tumors can be mediated through a number of different intracellular pathways (Extended Data Fig. 4).

Cellular mechanisms for Ppp2r2d

We next examined the cellular mechanisms driving T cell accumulation by a Ppp2r2d shRNA in tumors - specifically T cell infiltration, proliferation and apoptosis. T cell infiltration into tumors was assessed by transfer of OT-I CD8 T cells labeled with a cytosolic dye (carboxyfluorescein succinimidyl ester, CFSE). No differences were observed in the frequency of Ppp2r2d or LacZ shRNA-transduced CD8 T cells in tumors on day 1, arguing against a substantial effect on T cell infiltration (Fig. 3a). However, analysis of later time points (days 3–7) demonstrated a higher degree of proliferation (based on CFSE dilution) by Ppp2r2d compared to LacZ shRNA-transduced T cells (Fig. 3b, Extended Data Fig. 5a). The action of Ppp2r2d was downstream of T cell receptor activation because T cell proliferation was enhanced in tumors and to a lesser extent in tumor-draining lymph nodes (Extended Data Fig. 5a). In contrast, no proliferation was observed in irrelevant lymph nodes or the spleen where the relevant antigen was not presented to T cells (data not shown). Substantial T cell proliferation was even observed for LacZ shRNA-transduced T cells (complete dilution of CFSE dye by day 7), despite the presence of small numbers of such

cells in tumors. This suggested that LacZ shRNA-transduced T cells were lost by apoptosis. Indeed, a larger percentage of tumor-infiltrating T cells were labeled with an antibody specific for active caspase-3 when the LacZ control shRNA (rather than Ppp2r2d shRNA) was expressed (Fig. 3c, Extended Data Fig. 5b). Furthermore, co-culture of CD8 T cells with B16-Ova tumor cells showed that the majority of LacZ shRNA expressing T cells became apoptotic (65.7%) while most Ppp2r2d shRNA-transduced T cells were viable (89.5%, Fig. 3d).

These results suggested the possibility that Ppp2r2d shRNA-transduced CD8 T cells may be able to proliferate and survive even when they recognize their antigen directly presented by B16-Ova tumor cells. This idea was tested by implantation of tumor cells into *b2m−/−* mice which are deficient in expression of MHC class I proteins[34]. In such mice, only tumor cells but not professional antigen presenting cells of the host could present tumor antigens to T cells. Indeed, Ppp2r2d shRNA-transduced OT-I CD8 T cells showed massive accumulation within B16-Ova tumors in *b2m−/−* mice (Fig. 3e) while very small numbers of T cells were present in contralateral B16 tumors that lacked expression of the Ova antigen. Ppp2r2d-silenced T cells could thus effectively proliferate and survive in response to tumor cells, despite a lack of suitable co-stimulatory signals and an inhibitory microenvironment.

Ex vivo analysis of tumor-infiltrating T cells at a single-cell level using a nanowell device[35,36] also demonstrated that Ppp2r2d silencing increased cytokine production by T cells (Fig. 4a–c). T cells were activated for 3 hours by CD3/CD28 antibodies on lipid bilayers, followed by 1 hour cytokine capture on antibody-coated slides. CD8 T cells showed a higher secretion rate for IFNγ, IL-2 and GM-CSF, and a larger fraction of T cells more than one cytokine (Fig. 4b,c). The presence of larger numbers of IFNγ-producing T cells was confirmed by intracellular cytokine staining (Fig. 4d, Extended Data Fig. 5c).

PP2A represents a family of phosphatase complexes composed of catalytic, scaffolding and regulatory subunits. Cellular localization and substrate specificity are determined by one of many regulatory subunits of which Ppp2r2d is a member[32]. Ppp2r2d directs PP2A to Cdk1 substrates during interphase and anaphase; it thereby inhibits entry into mitosis and induces exit from mitosis[37]. PP2A also plays a gatekeeper role for BAD-mediated apoptosis. Phosphorylated BAD is sequestered in its inactive form in the cytosol by 14-3-3, while dephosphorylated BAD is targeted to mitochondria where it causes cell death by binding Bcl-X_L and Bcl-2[38]. PP2A phosphatases have also been shown to interact with the cytoplasmic domains of CD28 and CTLA-4 as well as Carma1 (upstream of the NF-κB pathway)[39,40], but it is not known which regulatory subunits are required for these activities; Ppp2r2d antibodies suitable for the required biochemical studies are currently not available.

Enhanced anti-tumor immunity

Finally, we assessed the ability of a Ppp2r2d shRNA to enhance the efficacy of adoptive T cell therapy. B16-Ova tumor cells (2×10^5) were injected subcutaneously into B6 mice. On day 12, mice bearing tumors of similar size were divided into seven groups, either receiving no T cells, 2×10^6 shRNA-transduced TRP-1 CD4 T cells, 2H-2K10^6 shRNA infected OT-I CD8 T cells, or both CD4 and CD8 T cells (days 12 and day 17). The modest anti-tumor

activity of OT-I CD8 T cells (expressing the control LacZ shRNA) is consistent with published data[41]. Ppp2r2d-silencing improved the therapeutic activity of both CD4 and CD8 T cells (Fig. 5a,b). A Ppp2r2d shRNA also enhanced anti-tumor responses when introduced into T cells specific for the endogenous melanoma antigens gp100 (pmel-1 CD8 T cells) and TRP-1 (TRP-1 CD4 T cells) (Fig. 5c). Gp100 is a relevant antigen in human melanoma, and a clinical trial in which a gp100-specific TCR (isolated from HLA-A2 transgenic mice) was introduced into peripheral blood T cells demonstrated therapeutic benefit in a subset of patients[42].

Ppp2r2d-silenced T cells acquired an effector phenotype in tumors (Extended Data Fig. 6a) and >30% of the cells expressed granzyme B (Extended Data Fig. 7a). Consistent with greatly increased numbers of such effector T cells in tumors (Extended Data Fig. 7b), TUNEL staining demonstrated increased apoptosis in tumors when Ppp2r2d rather than LacZ shRNA expressing T cells were present (Extended Data Fig. 7c). B16 melanomas are highly aggressive tumors in part because MHC class I expression is very low. Interestingly, Ppp2r2d but not LacZ shRNA-expressing T cells significantly increased MHC class I expression ($H\text{-}2K^b$) by tumor cells (Extended Data Fig. 7d), possibly due to the observed increase in IFNγ secretion by T cells (Fig. 4b–d). A Ppp2r2d shRNA did not reduce expression of inhibitory PD-1 or LAG-3 receptors on tumor-infiltrating T cells, demonstrating that its mechanism of action is distinct from these known negative regulators of T cell function (Extended Data Fig. 6b). This finding suggests combination approaches targeting these intracellular and cell surface molecules.

Discussion

These results establish the feasibility of *in vivo* discovery of novel targets for immunotherapy in complex tissue microenvironments. We show that it is possible to discover genes with differential action across tissues, as exemplified by T cell accumulation in tumors compared to secondary lymphoid organs. For genes with tissue-selective action, T cell proliferation and survival are likely to be under the control of the T cell receptor and therefore do not occur in tissues lacking presentation of a relevant antigen. Many variations of the approach presented here can be envisioned to investigate control of particular immune cell functions *in vivo*. For example, fluorescent reporters for expression of cytokines or cytotoxic molecules (granzyme B, perforin) could be integrated into our approach to discover genes that control critical T cell effector functions in tumors.

Targeting of key regulatory switches may offer new approaches to modify the activity of T cells in cancer and other pathologies. For example, recent clinical trials have shown that transfer of genetically modified T cells can result in substantial anti-tumor activity[43–46]. The efficacy of such T cell-based therapies could be enhanced by shRNA-mediated silencing of genes that inhibit T cell function in the tumor microenvironment.

Methods Summary

In vivo shRNA screening

Nine shRNA pools (~5 shRNAs per gene) were created and subcloned into the pLKO-Thy1.1 lentiviral vector. Each pool also included 85 negative-control shRNAs. OT-I T cells were cultured with IL-7 (5ng/mL) and IL-15 (100ng/mL); on day 2 cells were spin-infected with lentiviral pools supplemented with protamine sulfate (5μg/mL) in retronectin-coated 24-well plates (5μg/mL) at a multiplicity of infection (MOI) of 15. Following infection, OT-1 cells were cultured with IL-7 (2.5ng/mL), IL-15 (50ng/mL) and IL-2 (2ng/mL). On day 5, shRNA-transduced T cells were enriched by positive selection using the Thy1.1 surface reporter (Stemcell Technologies). T cells (5×10^6) were injected i.v. into C57BL/6 mice bearing day 14 B16-Ova tumors (15 mice per shRNA pool). Seven days later, shRNA-expressing T cells ($CD8^+V\alpha2^+V\beta5^+Thy1.1^+$) were isolated by flow cytometry from tumors, spleens, tumor-draining lymph nodes and irrelevant lymph nodes. Genomic DNA was purified (Qiagen) and deep-sequencing templates were generated by PCR amplification of the shRNA cassette. Representation of shRNAs in each pool was analyzed by deep sequencing using an Illumina Genome Analyzer[47].

Secondary screens were performed using focused pools containing ~15 shRNAs/gene as well as 85 negative controls. Cut-off in the secondary screen was defined as >3 shRNAs with >4 fold enrichment in tumor relative to spleen. Screening results were validated at a cellular level by introducing individual shRNAs into T cells, along with a reporter protein (GFP, TFP, RFP or Ametrine fluorescent proteins, Thy1.1). This approach enabled simultaneous testing of five shRNAs in an animal (three mice per group). Proliferation of shRNA-transduced T cells was visualized based on CFSE dilution after 24 hours as well as 3, 5 and 7 days.

Methods

In vivo shRNA screening

The study design was approved by the institutional animal care and use committee (IACUC). shRNAs targeting 255 genes over-expressed in dysfunctional T cells (anergic or exhausted state) and 1,307 kinase/phosphatase genes (~5 shRNAs per gene) were obtained from The RNAi Consortium (TRC; Broad Institute of MIT and Harvard, Cambridge, MA, USA). Nine pools were created and shRNAs subcloned into the pLKO-Thy1.1 lentiviral vector. Each pool also contained 85 negative-control shRNAs (number of shRNAs: GFP, 24; LacZ, 20; luciferase 25; RFP 16). OT-I T cells isolated by negative selection (Stemcell Technologies) were cultured with IL-7 (5ng/mL, Peprotech) and IL-15 (100ng/mL, Peprotech) in complete RPMI media (RPMI 1640, 10% FBS, 20mM HEPES, 1mM sodium pyruvate, 0.05mM 2-mercaptoethanol, 2mM L-glutamine, 100μg/ml streptomycin and 100μg/ml penicillin). On day 2, OT-I T cells (2×10^6/well) were spin-infected with lentiviral pools supplemented with protamine sulfate (5 μg/mL) in 24-well plates coated with retronectin (5μg/mL) at a multiplicity of infection (MOI) of 15. Typically ~50×10^6 OT-1 T cells were infected for each pool. Following infection, OT-I cells were cultured with IL-7 (2.5ng/mL), IL-15 (50ng/mL) and IL-2 (2ng/mL, BioLegend) in complete RPMI media. On

day 5, live cells were enriched using a dead cell removal kit (Miltenyi), and infected cells (20–25% Thy1.1+) were positively selected based on the Thy1.1 marker (Stemcell Technologies) to 50–60% Thy1.1 positivity. T cells (5×10^6) were injected i.v. into C57BL/6 mice bearing day 14 B16-Ova tumors (2×10^5 tumor cells injected on day 0), 15 mice per shRNA pool (number of animals chosen to provide sufficient cells for T cell isolation and PCR). Genomic DNA was isolated from 5×10^6 enriched OT-I cells as the start population for deep sequencing. Seven days later, shRNA-expressing T cells ($CD8^+V\alpha2^+V\beta5^+Thy1.1^+$) were isolated by flow cytometry from tumors, spleens, tumor-draining lymph nodes and irrelevant lymph nodes. Genomic DNA was isolated (Qiagen) and deep-sequencing templates were generated by PCR of the shRNA cassette. Representation of shRNAs in each pool was analyzed by deep sequencing using an Illumina Genome Analyzer[47]. Data were normalized using the average reads of control shRNAs in each pool. Kinase/phosphatase genes were selected for the secondary screen based on expression levels in T cells (Immunological Genome Project, http://www.immgen.org/). For the secondary screen, ~10 additional shRNAs were synthesized for each gene (IDT) for a total of ~15 shRNAs per gene. These focused pools contained 85 negative-control shRNAs. Two control shRNAs (one for RFP, one for luciferase) showed some enrichment in tumors relative to spleen (4.0 and 5.1-fold, respectively). Cut-off in the secondary screen was defined as >3 shRNA, with >4 fold enrichment in tumors relative to spleen. Data from primary and secondary screens are provided in Supplementary Table 1.

T cell isolation from tumors

B16-Ova melanomas were cut into small pieces in petri dishes containing 5mL of PBS, 2% FBS and washed with PBS. Tumors were resuspended in 15 mL RPMI supplemented with 2% FBS, 50U/mL Collagenase Type IV (Invitrogen), 20U/mL DNase (Roche); samples were incubated at 37° C for 2 hours, and tissue was further dissociated using a gentleMACS Dissociator (Miltenyi Biotech). Suspensions were washed three times with PBS and passed through a 70 μM strainer. Lymphocytes were isolated by density gradient centrifugation and then either analyzed or sorted by flow cytometry using a FACSAria (BD Biosciences).

Quantification of T cell enrichment in tumors by flow cytometry

Individual shRNAs were cloned into lentiviral vectors encoding five different reporter proteins (GFP, TFP, RFP or Ametrine fluorescent proteins, Thy1.1). Cytokine-pretreated OT-I T cells were transduced with lentiviral vectors driving expression of a single shRNA/reporter; 1×10^6 T cells of each population were mixed and co-injected i.v. into C57BL/6 mice bearing day 14 B16-Ova tumors. Seven days later, T cell populations were identified by flow cytometry based on co-introduced reporters. Fold-enrichment in tumors compared to spleen was calculated based on the percentage of OT-I T cells in each organ expressing a particular reporter. In other experiments, 2×10^6 OT-I CD8 or TRP-1 CD4 T cells were transduced with lentiviral vectors encoding Ppp2r2d or LacZ shRNAs (Thy1.1 reporter) and injected into mice bearing day 14 B16-Ova (for OT-I T cells) or B16 (for TRP-1 T cells) tumors. On day 7, absolute numbers of shRNA-expressing T cells were determined in tumors and spleens.

T cell migration, proliferation and cytokine secretion

OT-I T cells expressing LacZ or Ppp2r2d shRNAs were purified using the Thy1.1 reporter and cultured in complete RPMI media without added cytokines for 24 hours. Live cells isolated by Ficoll density gradient centrifugation (Sigma) were labeled with CFSE (carboxyfluorescein diacetate, succinimidyl ester, Invitrogen), and 2×10^6 labeled cells were injected into mice bearing day 14 B16-Ova tumors. CFSE dilution was quantified by flow cytometry at 24 hours as well as days 3, 5 and 7 following transfer. In addition, intracellular staining was performed on days 3, 5 and 7 for IFNγ, TNFα and isotype controls (BD).

T cell apoptosis

Cytokine pre-treated OT-I cells were transduced with LacZ or Ppp2r2d shRNAs and injected into mice bearing day 14 B16-Ova tumors. After 7 days, intracellular staining was performed using an activated caspase-3 antibody (Cell Signaling) and CD8/Thy1.1 double-positive T cells were gated in the FACS analysis.

Treatment of tumors by adoptive T cell transfer

B16-Ova cells (2×10^5) were injected s.c. into female C57BL/6 mice (10 weeks of age). On day 12, mice bearing tumors of similar size were divided into 7 groups (7–9 mice/group). Anti-CD3/CD28 bead activated CD4 TRP-1 or/and CD8 OT-I T cells infected with Ppp2r2d or LacZ shRNA vectors (2×10^6 T cells each) were injected i.v. on days 12 and day 17. For the treatment of B16 tumors, mice were treated at day 10 with anti-CD3/CD28 bead activated CD4 TRP-1 and CD8 pmel-1 T cells expressing Ppp2r2d or LacZ shRNAs (3×10^6 T cells each). Tumor size was measured every three days following transfer and calculated as length × width. Mice with tumors ≥20 mm on the longest axis were sacrificed.

Quantification of Ppp2r2d protein levels by mass spectrometry

A previously reported approach for absolute quantification (AQUA) of proteins from cell lysates by mass spectrometry was used to measure the effect of Ppp2r2d shRNA expression at the protein level[48]. This strategy is based on a ‘selective reaction monitoring’ approach in which a synthetic peptide with incorporated stable isotopes is used as an internal standard for mass spectrometry analysis. OT-I cells expressing LacZ or Ppp2r2d shRNAs were sorted to purity using FACS. Cells (1×10^6) were lysed in 1ml of MPER extraction reagent (Pierce) containing a Protease Inhibitor Cocktail (Sigma), 1mM EDTA and 1mM PMSF for 15 minutes on ice with occasional vortexing. Cell debris was removed by centrifugation and the protein supernatant was filtered (0.2μm SpinX centrifuge filter, Costar). Protein concentration was determined by Bradford assay (Biorad) and UV280 nm analysis (Nanodrop instrument); 0.1 mg of cellular protein was separated by SDS-PAGE and stained with Coomassie blue reagent (Pierce). Gel bands corresponding to a MW range of 45–60kDa were excised followed by in-gel digestion of proteins with trypsin. Eluted peptides were spiked with 300 fmol of isotopically labeled Ppp2r2d (FFEEPEDPSS[13C-15N-R]-OH) and Actin B (GYSFTTTAE[13C-15N-R]-OH) peptides (21^{st} Century Biochemicals) for quantification by LC-MS/MS (LTQ XL Orbitrap, Thermo Scientific). The Ppp2r2d peptide was chosen from a region of the protein that differs from other regulatory subunits of PP2A. Initially, a LC-MS/MS run of a LacZ shRNA sample was analyzed to localize the

Ppp2r2d and Actin B peptides that were being monitored. The AQUA peptides co-eluted with the corresponding endogenous peptides from the reverse-phase column, yet their higher MW (10 Da) enabled the ratio of peak intensity for endogenous and AQUA peptides to be determined using abundant peptide fragment ions. Triplicate samples were analyzed by SDS-PAGE - LC-MS/MS and statistical significance was determined using Graphpad Prism 6.0 software using a two-sided Student *t*-test (F test, * p=0.0062).

Extended Data

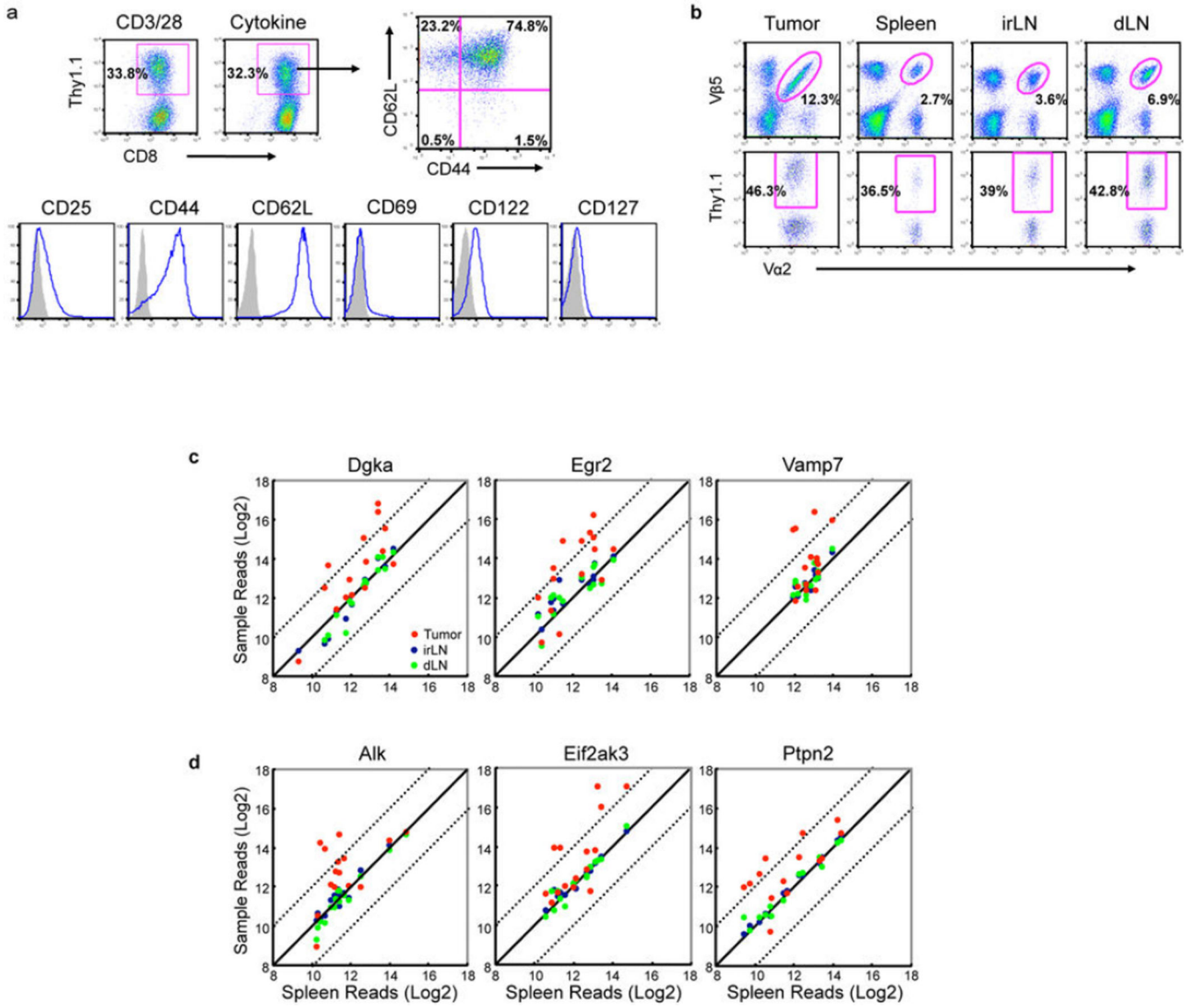

Extended Data Figure 1. *In vivo* RNAi screening procedure

a, Infection of $CD8^+$ T cells from $Rag1^{-/-}$/OT-I TCR transgenic mice with shRNA pools. T cells were either activated with anti-CD3/CD28 beads or exposed to recombinant murine IL-7/IL-15 for 48 hours. T cells were then infected with a LacZ control shRNA lentiviral vector and cultured for an additional three days. Transduction efficiency was determined

based on expression of the Thy1.1 reporter encoded by the lentiviral vector. Cytokine-cultured T cells expressing the LacZ control shRNA were then stained with a panel of activation markers (blue lines; isotype control, shaded). The majority of infected T cells exhibited a central memory phenotype ($CD62L^+CD44^+$). **b**, Representative flow cytometry plots of OT-I T cells sorted from tumors and secondary lymphoid organs for deep sequencing analysis (dLN, tumor-draining lymph node; irLN, irrelevant lymph node). $CD8^+V\alpha2^+V\beta5^+Thy1.1^+$ cells were sorted and genomic DNA was extracted for PCR amplification of the shRNA cassette. **c**, Deep sequencing results from T cell dysfunction screen. shRNA sequencing reads for genes positive in secondary screen are plotted in comparison to spleen for tumors (red), irrelevant lymph nodes (irLN, blue) and tumor-draining lymph nodes (dLN, green), with dashed lines indicating a deviation of $\log_2$ from the diagonal. Data show enrichment of particular shRNAs representing these genes in tumors compared to spleens or lymph nodes. **d**, Deep sequencing results from kinase and phosphatase screen, as described in (**c**).

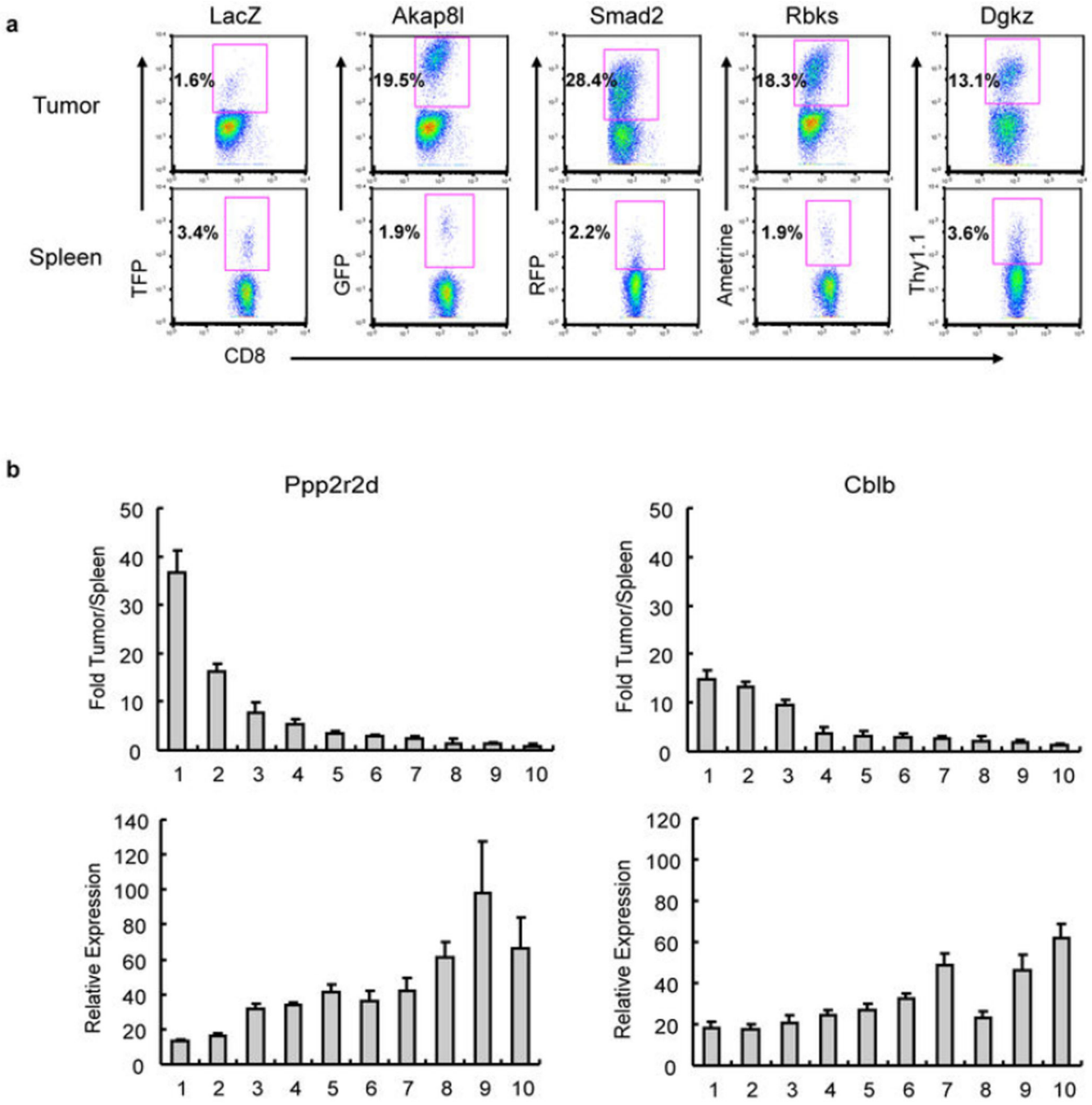

Extended Data Figure 2. Validation of shRNAs from *in vivo* RNAi screen

a, FACS-based analysis of T cell enrichment in tumors. Positive shRNAs from deep sequencing analysis were cloned into vectors driving expression of one of four distinct fluorescent proteins (TFP, GFP, RFP, Ametrine) or Thy1.1. OT-I T cells were transduced with shRNA vectors and the five populations of T cells (normalized for transduction efficiency) were co-injected into B16-Ova tumor-bearing mice. T cells were isolated from tumors and spleens on day 7, and the percentage of reporter-positive $CD8^+V\alpha2^+V\beta5^+$ T cells was determined by flow cytometry. **b**, FACS analysis of T cell enrichment in tumors

compared to spleen (as described above) for cells expressing a panel of Ppp2r2d or Cblb shRNAs (upper panels). Also, Ppp2r2d and Cblb mRNA levels were measured by qPCR prior to T cell transfer (lower panels). The strongest T cell enrichment in tumors was observed for shRNAs with >80% knock-down efficiency at the mRNA level (shRNAs #1 and 2 for both Ppp2r2d and Cblb). Data represent biological replicates (n=3), each value represents mean +/− s.d.

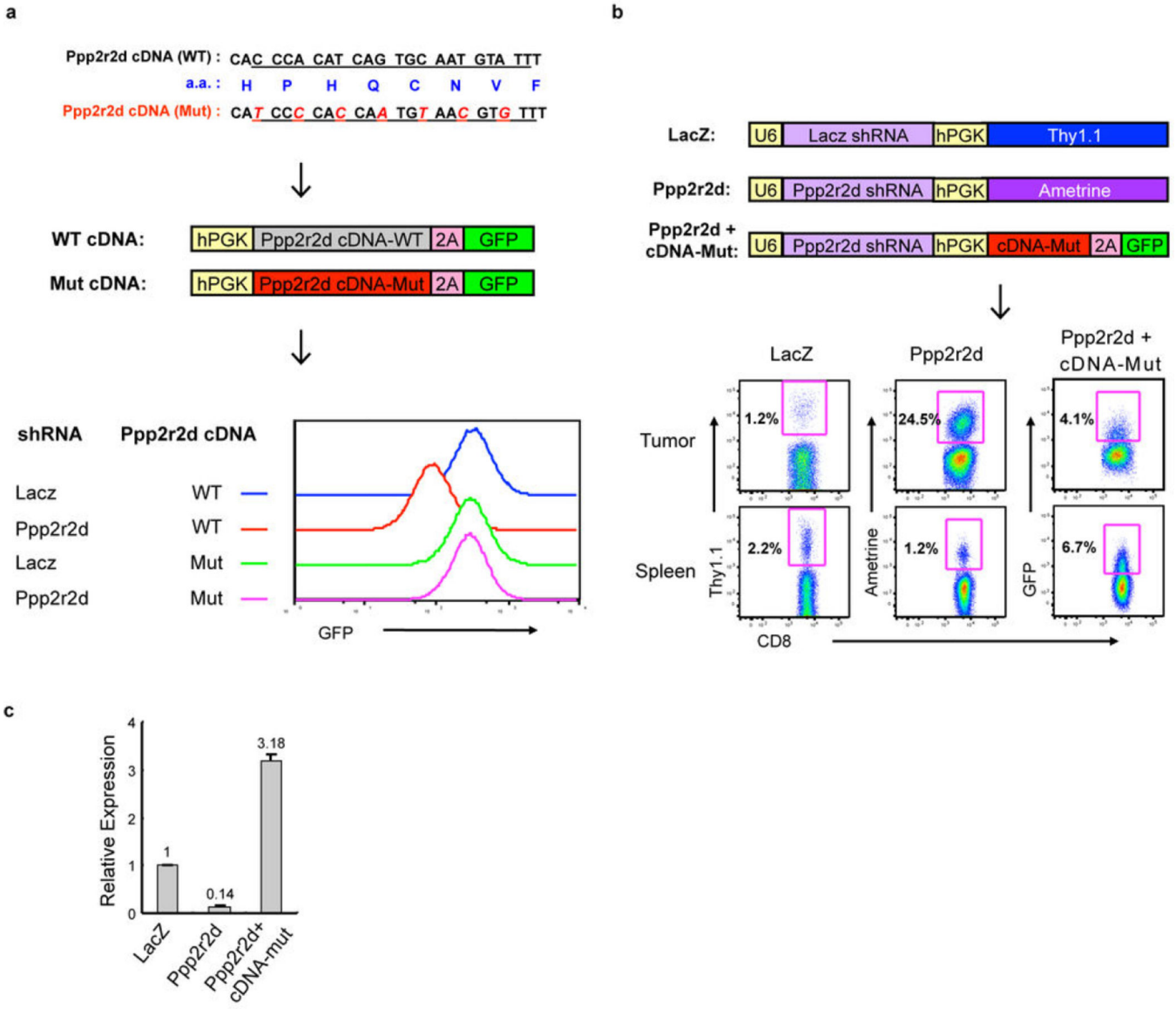

Extended Data Figure 3. Specificity of Ppp2r2d shRNA

a, Generation of mutant Ppp2r2d cDNA with wild-type protein sequence but disrupted shRNA binding site. Both mutant and wild-type Ppp2r2d cDNAs were cloned into a modified pLKO.3G vector with a 2A peptide ribosomal skip sequence and GFP. This approach resulted in stoichiometric expression of Ppp2r2d protein and GFP in EL4 thymoma cells. GFP-expressing EL4 cells were sorted to purity and transduced with LacZ or

Ppp2r2d shRNA vectors expressing a Thy1.1 reporter. shRNA-transduced (Thy1.1$^+$) cells were analyzed by flow cytometry for GFP expression. The Ppp2r2d shRNA reduced GFP levels when wild-type Ppp2r2d cDNA, but not when mutant Ppp2r2d cDNA was co-expressed. **b**, Expression of Ppp2r2d mutant cDNA prevents phenotype induced by Ppp2r2d shRNA. OT-I T cells were transduced with a vector encoding LacZ shRNA, Ppp2r2d shRNA or Ppp2r2d shRNA plus mutant Ppp2r2d cDNA. The different cell populations were normalized for transduction efficiency and co-injected into B16-Ova tumor-bearing mice. The percentage of each T cell population in tumors and spleens was quantified by gating on CD8$^+$Vα2$^+$Vβ5$^+$ T cells; transduced cells were detected based on expression of Thy1.1 or Ametrine/GFP fluorescent reporters (representative data from 2 independent experiments, n=3 mice per experiment). **c**, qPCR analysis for Ppp2r2d expression in OT-I T cells transduced with LacZ shRNA, Ppp2r2d shRNA, and Ppp2r2d shRNA plus Ppp2r2d mutant cDNA. Data represent biological replicates (n=3), each value represents mean +/− s.d.

a

Gene Symbol	Function	Enrichment Fold
Ppp2r2d	Regulatory subunit of PP2A phosphatase	17.2
Arhgap5	Negative regulator of Rho GTPases	15.7
Alk	Anaplastic lymphoma kinase (translocation of nucleophosmin and ALK in ALCL)	13.5
Egr2	Transcription factor involved in T cell unresponsiveness, expression of Cblb	10.2
Ptpn2	Inhibitor of T cell and cytokine signaling	7.4

b

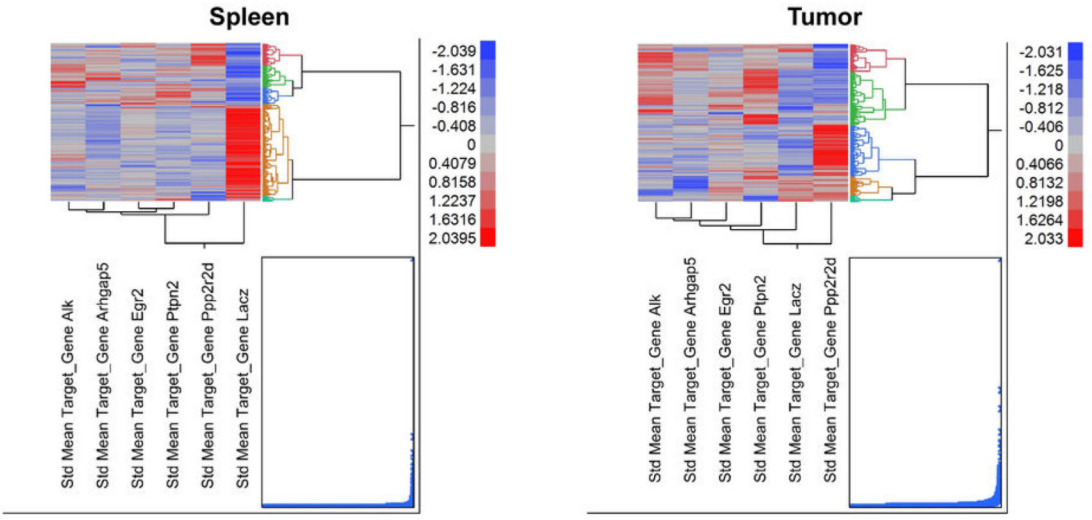

c

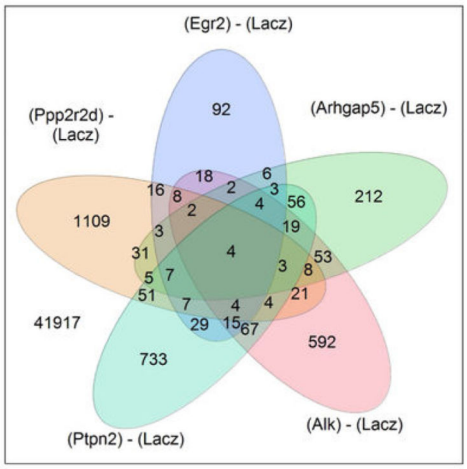

	Alk	Arhgap5	Egr2	Ppp2r2d	Ptpn2
Alk		1.0E-31	5.6E-14	ns	1.9E-23
Arhgap5			7.8E-07	9.5E-14	3.5E-16
Egr2				3.2E-08	3.3E-24
Ppp2r2d					1.6E-07
Ptpn2					

Extended Data Figure 4. Expression profiles of gene-silenced CD8 T cells in tumors

OT-I T cells were transduced with lentiviral vectors driving expression of one of five experimental shRNAs or LacZ control shRNA. T cells were injected into day 14 B16-Ova tumor-bearing mice and isolated from tumors and spleens 7 days later. Cells were sorted to high purity and total RNA was obtained for Affymetrix gene expression profiling. For each shRNA, arrays were performed in triplicate (6 mice per group). **a**, Two genes (Egr2 and Ptpn2) have known functions in T cells. Enrichment in tumor versus spleen was calculated based on deep sequencing results from the secondary screen. **b**, Clustering of mean

expression levels for mRNAs found to be significantly regulated by T cells in spleens or tumors expressing the LacZ control shRNA or one of five experimental shRNAs. Significant expression differences were defined as an Anova *P* value ≤0.01 between T cells expressing LacZ control shRNA or one of five experimental shRNAs (Alk, Arhgap5, Egr2, Ptpn2 or Ppp2r2d) (JMP-Genomics 6.0, SAS Institute Inc.). mRNAs significantly regulated in one or more treatment groups are shown after clustering (Fast Ward). **c**, Venn diagram showing overlaps between expression signatures by tumor-infiltrating T cells transduced with one of the five experimental shRNAs (signatures defined as an Anova $p \leq 0.01$ as described above). Indicated are the numbers of overlapping probe IDs for any combination of the 5 signatures, as indicated by the overlapping ovals. The significance of the overlaps versus those expected by random chance (Fishers Exact Test) is shown in the accompanying table.

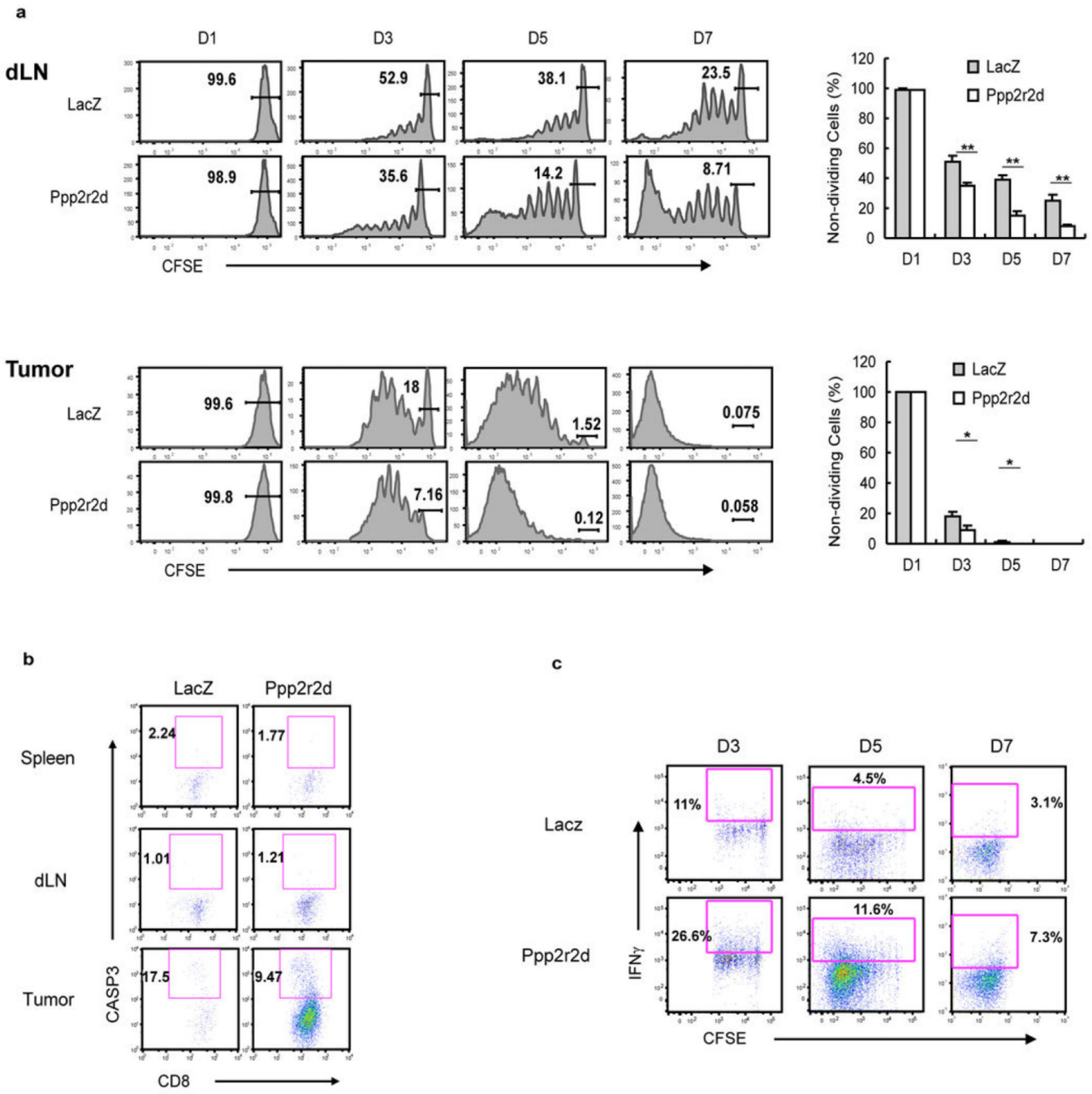

Extended Data Figure 5. Ppp2r2d shRNA enhances T cell proliferation and reduces apoptosis

a, Proliferation of Ppp2r2d shRNA-expressing T cells in tumors and tumor-draining lymph nodes. OT-I T cells expressing Ppp2r2d or LacZ shRNAs were labeled with CFSE and injected into B16-Ova tumor-bearing mice. T cells were isolated from the indicated organs on days 1, 3, 5 and 7 to examine the extent of T cell proliferation based on CFSE dilution. T cells that had not diluted CFSE (nondividing cells) were quantified (right). **b,** Viability of tumor-infiltrating T cells. OT-I T cells expressing Pp2r2d or LacZ shRNAs were injected into B16-Ova tumor-bearing mice. T cells were isolated on day 7 and apoptosis was

assessed by intracellular staining with an antibody specific for activated caspase-3 (some T cell death may have been caused by the isolation procedure from tumors). **c,** Intracellular cytokine staining for IFNγ by LacZ and Ppp2r2d shRNA-expressing T cells harvested from B16-Ova tumors (primary flow cytometry analysis for data summarized in Figure 4d); T cells were labeled with CFSE prior to injection. Data for all experiments are representative of two independent trials. Statistical analysis was performed on biological replicates (n=3); * $P \leq 0.05$, ** $P \leq 0.01$, two-sided Student's *t*-test. Each value represents mean +/− s.d.

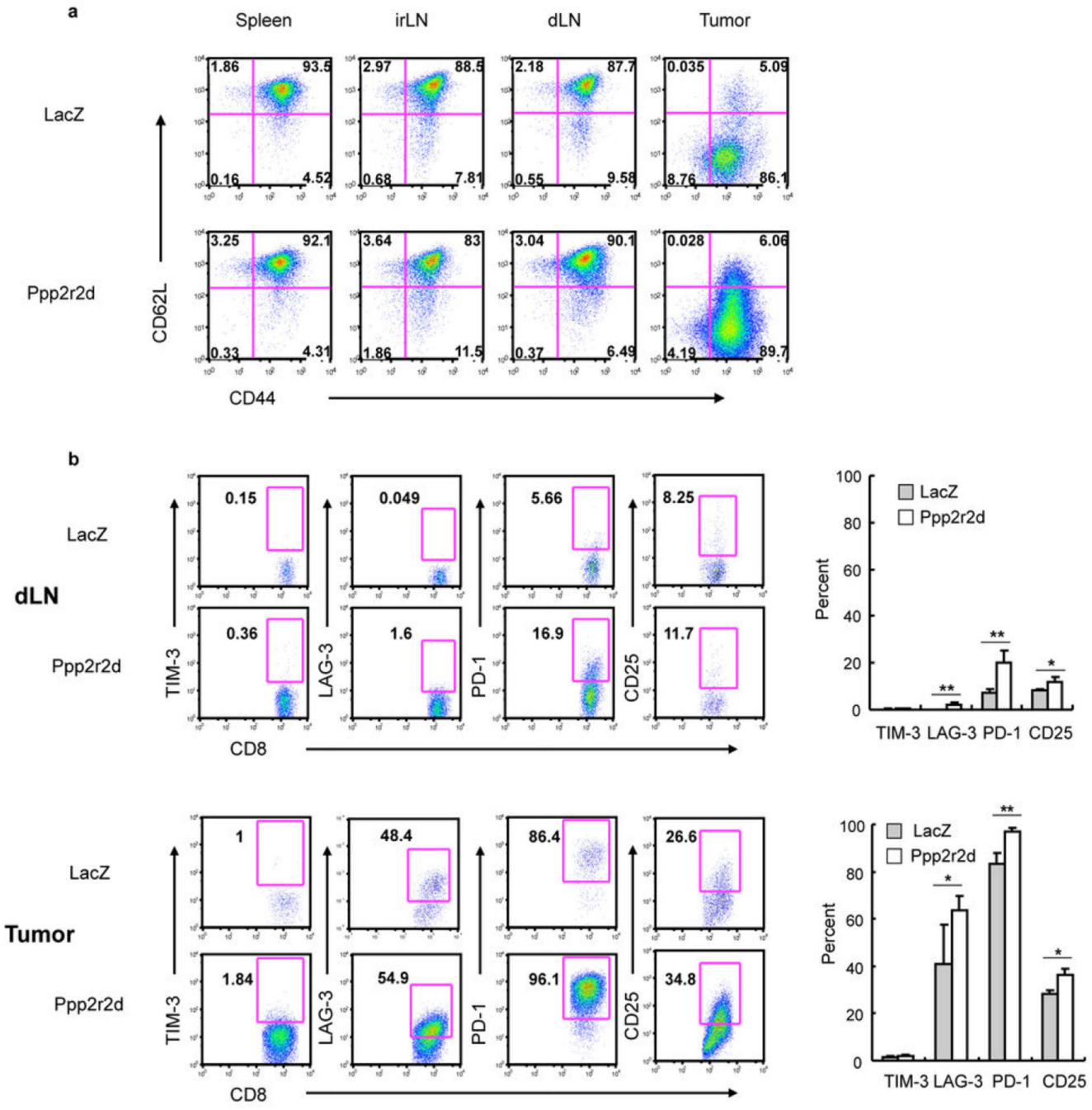

Extended Data Figure 6. Phenotypic characterization using memory, activation and exhaustion markers

a, The majority of adoptively transferred OT-I cells have a memory phenotype in lymph nodes but an effector phenotype in tumors. Cytokine pre-treated cells expressing Ppp2r2d or LacZ shRNAs were injected into mice bearing day 14 B16-Ova tumors. On day 7 following transfer, T cells were harvested from the indicated organs and stained with CD62L and CD44 antibodies. FACS analysis of shRNA-expressing OT-I cells was performed by gating on CD8/Thy1.1 double-positive cells. **b,** Analysis of exhaustion markers. OT-I cells were harvested from draining lymph nodes and tumors of mice and stained with antibodies specific for TIM-3, LAG-3, PD-1 and CD25. For all experiments (n=3 biological replicates; * $P \leq 0.05$, ** $P \leq 0.01$, Two-sided Student's *t*-test); each value represents mean +/− s.d.

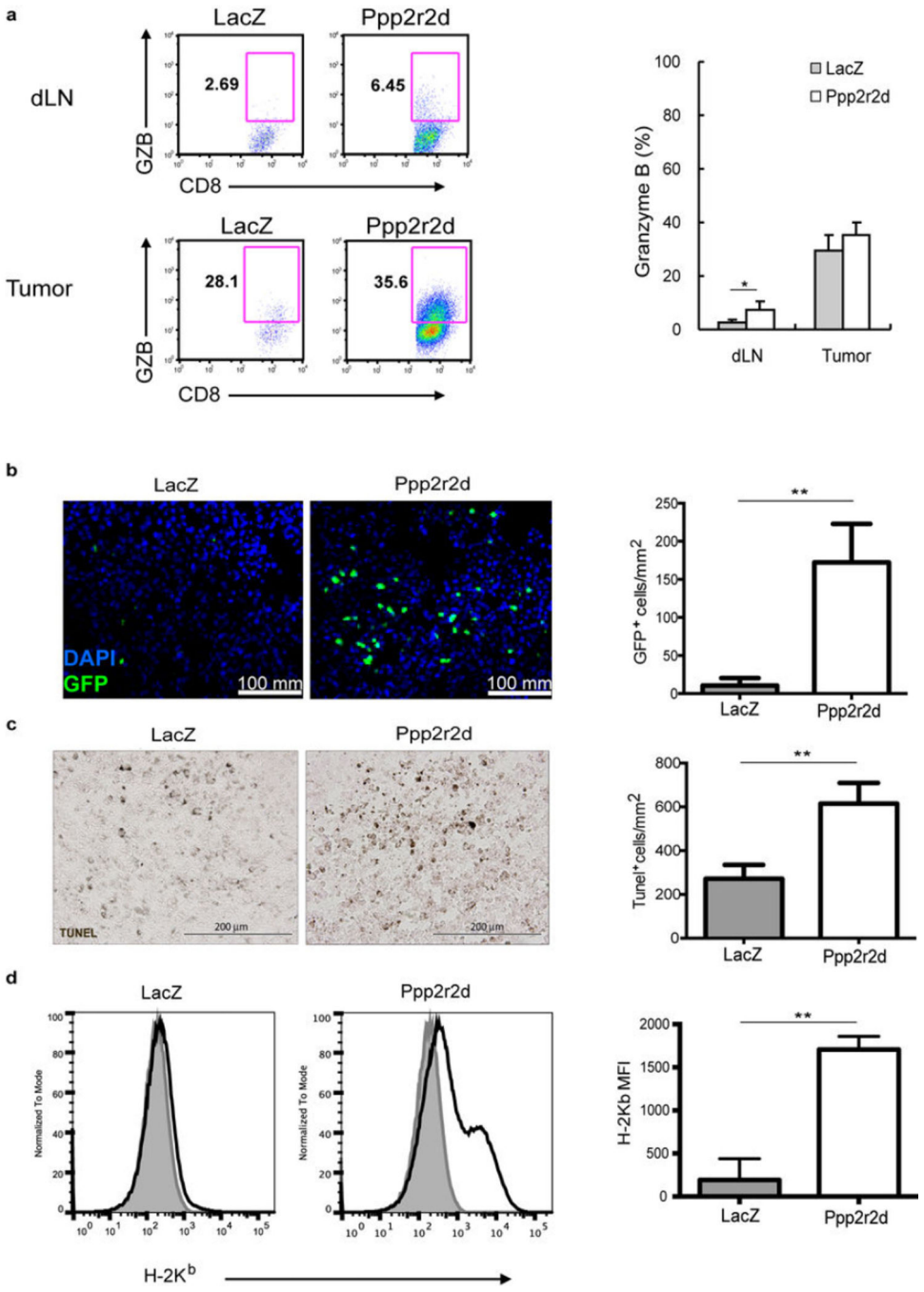

Extended Data Figure 7. Mechanisms of anti-tumor activity of Ppp2r2d-silenced T cells

a, Intracellular staining for granzyme B by OT-I T cells in tumor-draining lymph nodes and tumors. **b,** Infiltration of shRNA-expressing T cells into tumors. OT-I T cells were transduced with LacZ or Ppp2r2d shRNA vectors encoding a GFP reporter and injected into B16-Ova tumor-bearing mice. After 7 days, tumors were excised and frozen sections stained with anti-GFP and DAPI to enumerate shRNAexpressing OT-I T cells in tumors. **c,** Tumor cell apoptosis. TUNEL immunohistochemistry was performed on tissue sections and apoptotic cells were quantified. **d,** MHC class I expression by tumor cells. Tumors were

digested with collagenase and stained with CD45.2 and H-2K^b antibodies. FACS analysis for H-2K^b expression was performed by gating on CD45.2-negative melanoma cells. Data represent biological replicates (n=3), each value represents mean +/− s.d.

Extended Data Table 1
Tumor-enriched shRNAs from secondary screen

Secondary screens were performed with a total of ~15 shRNAs for each gene of interest. **a**, Results from secondary screen of T cell dysfunction pool shRNA library. Genes for which at least 3 shRNAs showed ≥4 fold enrichment in tumors are listed, along with a brief description of their function. **b**, Results from secondary screen of kinase and phosphatase shRNA libraries.

a

	Symbol	Total # shRNAs	Enrichment (fold)	Function
1	Dgkz	6	5.2 – 14.0	Phosphorylates and thereby inactivates DAG
2	Egr2	6	4.0 – 10.2	Transcription factor involved in T cell unresponsiveness, expression of Cblb
3	Smad2	5	6.7 – 30.3	TGF beta signaling pathway
4	Cblb	5	4.1 – 10.8	E3 ubiquitin ligase (degradation of TCR and signaling molecules; ko mice reject tumors
5	Inpp5b	5	4.3 – 9.5	Inositol polyphosphate-5-phosphatase, hydrolyzes PIP2
6	Socs1	5	4.1 – 8.5	Inhibitor of cytokine signaling
7	Jun	5	5.2 – 6.4	Persistent AP-1 activation in turn or-infiltrating T cells leads to upregulated PD-1
8	Vamp7	4	4.0 – 11.3	Vesicle associated transmembrane protein
9	Dgka	4	5.0 – 10.2	Phosphorylates and thereby inactivates DAG
10	Mdfic	4	4.4 – 10.0	Inhibits viral gene expression, interacts with cyclin T1 and T2
11	Nptxr	4	4.0 – 7.2	Pentraxin Receptor
12	Socs3	4	4.6 – 6.3	Inhibitor of cytokine signaling
13	Entpd1	3	6.5 – 13.3	Extracellular degradation of ATP to AMP {an inhibitory signal through AMP kinase)
14	Pdz1lp1	3	4.8 – 12.9	Pdzk1 interacting protein, expression correlates with tumor progression
15	F11r	3	4.6 – 6.8	Cell Migration
16	Fyn	3	4.1 – 6.5	Inhibits activation of resting T cells (through Csk)
17	Ypel2	3	4.6 – 5.1	Function unknown

b

	Symbol	Total # shRNAs	Enrichment (fold)	Function
1	Rbks	6	4.0 – 12.8	Ribokinase, carbohydrate metabolism
2	Pkd1	6	4.9 – 9.9	Cell cycle arrest (activates JAK/STAT pathway)
3	Ppp2r2d	5	4.0 – 17.2	Regulatory subunit of PP2A phosphatase
4	Eif2ak3	5	4.8 – 13.4	ER stress sensor, resistance of cancer cells to chemotherapy

b

	Symbol	Total # shRNAs	Enrichment (fold)	Function
5	Ptpn2	5	4.7 – 7.4	Inhibitor of T cell and cytokine signaling
6	Hipk1	4	4.5 – 12.3	Interacts with p53 and c-myb, knockout mice develop fewer carcinogen-induced tumors
7	Grk6	4	4.2 – 11	Regulator of particular G-protein coupled receptors
8	Cdkn2a	4	4.1 – 7.2	G1 cell cycle arrest and apoptosis in T cells
9	Sbf1	4	4.8 – 6.9	Activates MTMR2, which dephosphorylates PI(3)P and PI(3,5)P2
10	Ipmk	4	4.0 – 6.9	Inositol polyphosphate kinase, nuclear functions such as chromatin remodeling
11	Rock1	4	4.1 – 6.5	Rho kinase, inhibitors have shown activity in mouse models of cancer
12	Stk17b	4	4.0 – 6.4	Inhibitor of T cell signaling forms complex with protein kinase D
13	Mast2	4	4.1 – 5.1	Microtubule-associated serine/threonine kinase
14	Arhgap5	3	6.0 – 15.7	Negative regulator of Rho GTPases, inhibition can reduce cancer cell invasion
15	Alk	3	9.6 – 13.5	Anaplastic lymphoma kinase (translocation of nucleophosmin and ALK in ALCL)
16	Nuak	3	4.5 – 13.1	Member of AMP-activated protein kinase-related kinase family, oncogene in melanoms
17	Akap8l	3	4.4 – 11.8	A-kinase anchoring protein, recruits cAMP-dependent protein kinase (PKA) to chromatin
18	Pdp1	3	4.1 – 9.8	Pyruvate dehydrogenase phosphatase 1, regulation of glucose metabolism
19	Yes1	3	5.4 – 9.7	Src family kinase, oncogene in several tumors
20	Met	3	4.1 – 8.9	Receptor tyrosine kinase, involved in hepatocellular and other cancers
21	Ppm1g	3	6.2 – 8.2	Dephosphorylates spliceosome substrates and histones H2A-H2B
22	Blvrb	3	5.3 – 8.0	Biliverdin reductase, also transcription factor, arrest of cell cycle
23	Tnk1	3	5.2 – 7.6	Downregulates Ras pathway (phosphorylation of Grb2), inhibition of NF-kB pathway
24	Prkab2	3	4.1 – 7.0	Subunit of AMP kinase, inhibits fatty acid synthesis and mTOR pathway
25	Trpm7	3	4.9 – 5.9	Ion channel and serine-threonine kinase
26	Ppp3cc	3	4.2 – 4.4	Regulatory subunit of calcineurin (phosphatase in T cell receptor signaling)

Supplementary Material

Refer to Web version on PubMed Central for supplementary material.

Acknowledgements

This work was supported by the National Institutes of Health (Transformative Research Award 1R01CA173750 to K.W.W.), the Melanoma Research Alliance (to K.W.W.), the DF/HCC – MIT Bridge Project and the Lustgarten Foundation (to K.W.W., J.C.L. and H.P.), Novartis Institutes of Biomedical Research (to K.W.W.), the Koch Institute Support Grant P30-CA14051 from the National Cancer Institute, the American Cancer Society John W. Thatcher, Jr. Postdoctoral Fellowship in Melanoma Research (to D.S.), the Terri Brodeur Breast Cancer Foundation Postdoctoral Fellowship (to P.Z.) and a NIH T32 grant (AI07386 to D.A.A.A.).

References

1. Galon J, et al. Type, density, and location of immune cells within human colorectal tumors predict clinical outcome. Science. 2006; 313:1960–1964. [PubMed: 17008531]
2. Hamanishi J, et al. Programmed cell death 1 ligand 1 and tumor-infiltrating CD8+ T lymphocytes are prognostic factors of human ovarian cancer. Proceedings of the National Academy of Sciences of the United States of America. 2007; 104:3360–3365. [PubMed: 17360651]
3. Mahmoud SM, et al. Tumor-Infiltrating CD8+ Lymphocytes Predict Clinical Outcome in Breast Cancer. J Clin Oncol. 2011; 29:1949–1955. [PubMed: 21483002]
4. Bindea G, et al. Spatiotemporal dynamics of intratumoral immune cells reveal the immune landscape in human cancer. Immunity. 2013; 39:782–795. [PubMed: 24138885]
5. Matsushita H, et al. Cancer exome analysis reveals a T-cell-dependent mechanism of cancer immunoediting. Nature. 2012; 482:400–404. [PubMed: 22318521]
6. Oble DA, Loewe R, Yu P, Mihm MC Jr. Focus on TILs: prognostic significance of tumor infiltrating lymphocytes in human melanoma. Cancer Immun. 2009; 9:3. [PubMed: 19338264]
7. DuPage M, Mazumdar C, Schmidt LM, Cheung AF, Jacks T. Expression of tumour-specific antigens underlies cancer immunoediting. Nature. 2012; 482:405–409. [PubMed: 22318517]
8. Schreiber RD, Old LJ, Smyth MJ. Cancer immunoediting: integrating immunity's roles in cancer suppression and promotion. Science. 2011; 331:1565–1570. [PubMed: 21436444]
9. Pages F, et al. In situ cytotoxic and memory T cells predict outcome in patients with early-stage colorectal cancer. J Clin Oncol. 2009; 27:5944–5951. [PubMed: 19858404]
10. Rusakiewicz S, et al. Immune infiltrates are prognostic factors in localized gastrointestinal stromal tumors. Cancer research. 2013; 73:3499–3510. [PubMed: 23592754]
11. Stumpf M, et al. Intraepithelial CD8-positive T lymphocytes predict survival for patients with serous stage III ovarian carcinomas: relevance of clonal selection of T lymphocytes. Br J Cancer. 2009; 101:1513–1521. [PubMed: 19861998]
12. Gabrilovich DI, Nagaraj S. Myeloid-derived suppressor cells as regulators of the immune system. Nat Rev Immunol. 2009; 9:162–174. [PubMed: 19197294]
13. Shiao SL, Ganesan AP, Rugo HS, Coussens LM. Immune microenvironments in solid tumors: new targets for therapy. Genes Dev. 2011; 25:2559–2572. [PubMed: 22190457]
14. Tanchot C, et al. Tumor-infiltrating regulatory T cells: phenotype, role, mechanism of expansion in situ and clinical significance. Cancer Microenviron. 2013; 6:147–157. [PubMed: 23104434]
15. Hodi FS, et al. Improved Survival with Ipilimumab in Patients with Metastatic Melanoma. N Engl J Med. 2011
16. Topalian SL, et al. Safety, Activity, and Immune Correlates of Anti-PD-1 Antibody in Cancer. The New England journal of medicine. 2012
17. Brahmer JR, et al. Safety and activity of anti-PD-L1 antibody in patients with advanced cancer. The New England journal of medicine. 2012; 366:2455–2465. [PubMed: 22658128]
18. Leach DR, Krummel MF, Allison JP. Enhancement of antitumor immunity by CTLA-4 blockade. Science. 1996; 271:1734–1736. [PubMed: 8596936]
19. Wolchok JD, et al. Nivolumab plus ipilimumab in advanced melanoma. The New England journal of medicine. 2013; 369:122–133. [PubMed: 23724867]
20. Curran MA, Montalvo W, Yagita H, Allison JP. P-1 and CTLA-4 combination blockade expands infiltrating T cells and reduces regulatory T and myeloid cells within B16 melanoma tumors. Proceedings of the National Academy of Sciences of the United States of America. 2010; 107:4275–4280. [PubMed: 20160101]
21. Westbrook TF, et al. A genetic screen for candidate tumor suppressors identifies REST. Cell. 2005; 121:837–848. [PubMed: 15960972]
22. Zender L, et al. An oncogenomics-based in vivo RNAi screen identifies tumor suppressors in liver cancer. Cell. 2008; 135:852–864. [PubMed: 19012953]
23. Luo B, et al. Highly parallel identification of essential genes in cancer cells. Proceedings of the National Academy of Sciences of the United States of America. 2008; 105:20380–20385. [PubMed: 19091943]

24. Fidler IJ. Biological behavior of malignant melanoma cells correlated to their survival in vivo. Cancer research. 1975; 35:218–224. [PubMed: 1109790]
25. Hogquist KA, et al. T cell receptor antagonist peptides induce positive selection. Cell. 1994; 76:17–27. [PubMed: 8287475]
26. Bellone M, et al. Relevance of the tumor antigen in the validation of three vaccination strategies for melanoma. Journal of immunology. 2000; 165:2651–2656.
27. Overwijk WW, et al. Tumor regression and autoimmunity after reversal of a functionally tolerant state of self-reactive CD8+ T cells. The Journal of experimental medicine. 2003; 198:569–580. [PubMed: 12925674]
28. Paolino M, Penninger JM. Cbl-b in T-cell activation. Semin Immunopathol. 2010; 32:137–148. [PubMed: 20458601]
29. Zheng Y, Zha Y, Gajewski TF. Molecular regulation of T-cell anergy. EMBO Rep. 2008; 9:50–55. [PubMed: 18174897]
30. Doody KM, Bourdeau A, Tremblay ML. T-cell protein tyrosine phosphatase is a key regulator in immune cell signaling: lessons from the knockout mouse model and implications in human disease. Immunological reviews. 2009; 228:325–341. [PubMed: 19290937]
31. Tamiya T, Kashiwagi I, Takahashi R, Yasukawa H, Yoshimura A. Suppressors of cytokine signaling (SOCS) proteins and JAK/STAT pathways: regulation of T-cell inflammation by SOCS1 and SOCS3. Arterioscler Thromb Vasc Biol. 2011; 31:980–985. [PubMed: 21508344]
32. Barr FA, Elliott PR, Gruneberg U. Protein phosphatases and the regulation of mitosis. J Cell Sci. 2011; 124:2323–2334. [PubMed: 21709074]
33. Muranski P, et al. Tumor-specific Th17-polarized cells eradicate large established melanoma. Blood. 2008; 112:362–373. [PubMed: 18354038]
34. Koller BH, Marrack P, Kappler JW, Smithies O. Normal development of mice deficient in beta 2M, MHC class I proteins, and CD8+ T cells. Science. 1990; 248:1227–1230. [PubMed: 2112266]
35. Torres AJ, Contento RL, Gordo S, Wucherpfennig KW, Love JC. Functional single-cell analysis of T-cell activation by supported lipid bilayer-tethered ligands on arrays of nanowells. Lab Chip. 2013; 13:90–99. [PubMed: 23070211]
36. Han Q, Bradshaw EM, Nilsson B, Hafler DA, Love JC. Multidimensional analysis of the frequencies and rates of cytokine secretion from single cells by quantitative microengraving. Lab Chip. 2010; 10:1391–1400. [PubMed: 20376398]
37. Mochida S, Maslen SL, Skehel M, Hunt T. Greatwall phosphorylates an inhibitor of protein phosphatase 2A that is essential for mitosis. Science. 2010; 330:1670–1673. [PubMed: 21164013]
38. Chiang CW, et al. Protein phosphatase 2A dephosphorylation of phosphoserine 112 plays the gatekeeper role for BAD-mediated apoptosis. Mol Cell Biol. 2003; 23:6350–6362. [PubMed: 12944463]
39. Chuang E, et al. The CD28 and CTLA-4 receptors associate with the serine/threonine phosphatase PP2A. Immunity. 2000; 13:313–322. [PubMed: 11021529]
40. Eitelhuber AC, et al. Dephosphorylation of Carma1 by PP2A negatively regulates T-cell activation. Embo J. 2011; 30:594–605. [PubMed: 21157432]
41. Tao J, et al. JNK2 negatively regulates CD8+ T cell effector function and anti-tumor immune response. Eur J Immunol. 2007; 37:818–829. [PubMed: 17301952]
42. Johnson LA, et al. Gene therapy with human and mouse T-cell receptors mediates cancer regression and targets normal tissues expressing cognate antigen. Blood. 2009; 114:535–546. [PubMed: 19451549]
43. Brenner MK, Heslop HE. Adoptive T cell therapy of cancer. Current opinion in immunology. 2010; 22:251–257. [PubMed: 20171074]
44. Turtle CJ, Hudecek M, Jensen MC, Riddell SR. Engineered T cells for anti-cancer therapy. Current opinion in immunology. 2012; 24:633–639. [PubMed: 22818942]
45. Kalos M, June CH. Adoptive T cell transfer for cancer immunotherapy in the era of synthetic biology. Immunity. 2013; 39:49–60. [PubMed: 23890063]
46. Restifo NP, Dudley ME, Rosenberg SA. Adoptive immunotherapy for cancer: harnessing the T cell response. Nature reviews. Immunology. 2012; 12:269–281.

47. Ashton JM, et al. Gene sets identified with oncogene cooperativity analysis regulate in vivo growth and survival of leukemia stem cells. Cell Stem Cell. 2012; 11:359–372. [PubMed: 22863534]

48. Gerber SA, Rush J, Stemman O, Kirschner MW, Gygi SP. Absolute quantification of proteins and phosphoproteins from cell lysates by tandem MS. Proceedings of the National Academy of Sciences of the United States of America. 2003; 100:6940–6945. [PubMed: 12771378]

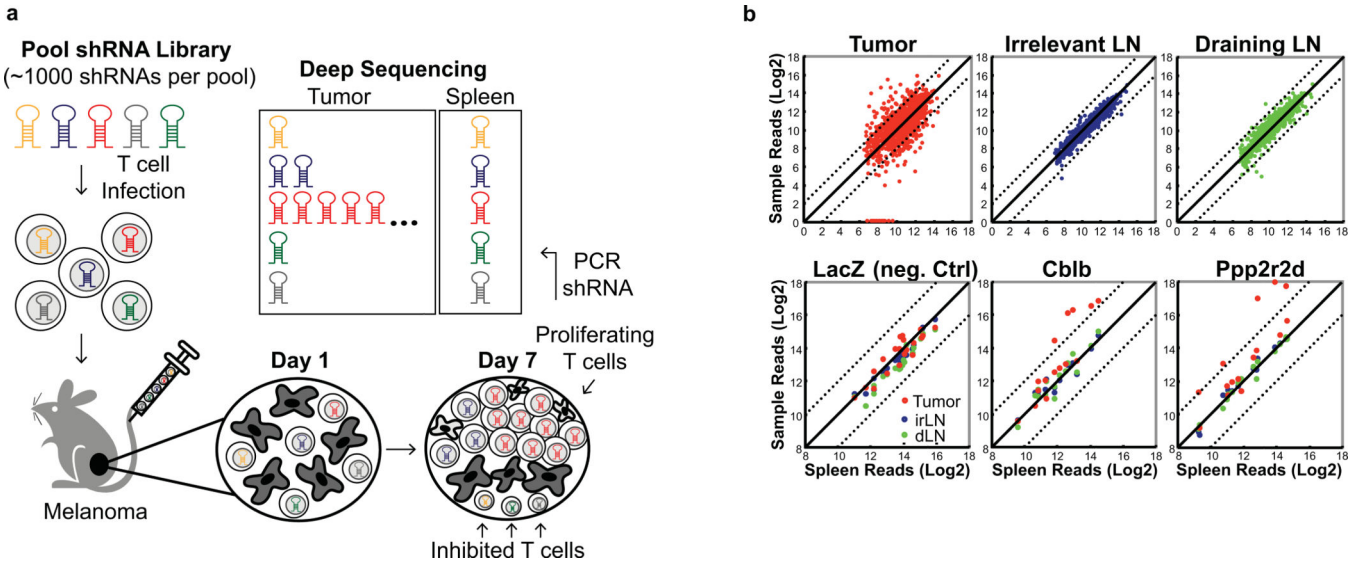

Figure 1. *In vivo* RNAi discovery of immunotherapy targets

a *In vivo* discovery approach for negative regulators of T cell function in tumors. T cells infected with shRNA libraries were injected into tumor-bearing mice; shRNAs that enabled T cell accumulation in tumors were identified by deep sequencing of the shRNA cassette from purified T cells. **b**, Deep sequencing data: shRNA sequence reads from tumors, irrelevant (irLN) and draining lymph nodes (dLN) versus spleen. Upper row: sequence reads for all genes in a pool, lower row: individual genes (LacZ, negative control). Dashed lines indicate a deviation by $\log_2$ from diagonal.

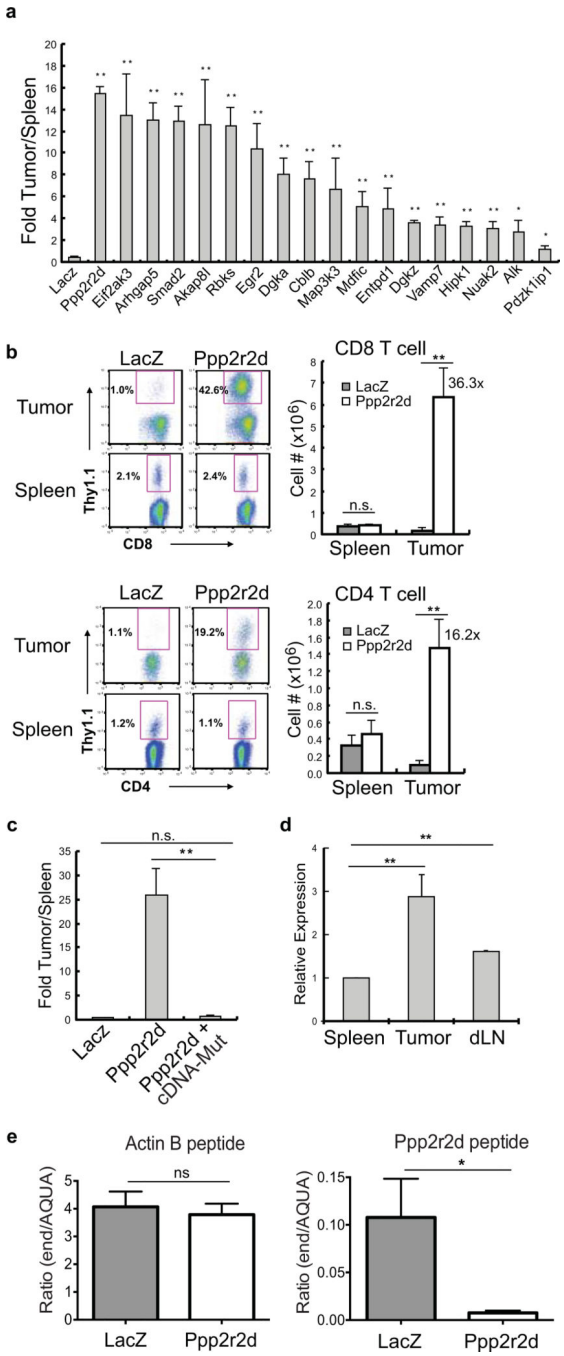

Figure 2. shRNA-driven accumulation of T cells in B16 melanoma

a, CD8 (OT-I) T cell enrichment in tumors relative to spleen (n=3). **b**, Enrichment of Ppp2r2d-silenced CD8 (OT-I) or CD4 (TRP1) T cells (Thy1.1$^+$ cells) in tumor versus spleen. **c**, Reversal of shRNA-induced phenotype by Ppp2r2d cDNA with mutated shRNA binding site. **d**, qPCR for Ppp2r2d mRNA in tumor-infiltrating OT-I T cells (day 7). **e**, Ppp2r2d protein quantification by mass spectrometry with labeled synthetic peptides (AQUA, ratio of endogenous to AQUA peptides). Representative data from two independent experiments (a–d); Two-sided student's *t*-test, * $P<0.05$, ** $P<0.01$; mean +/− s.d.

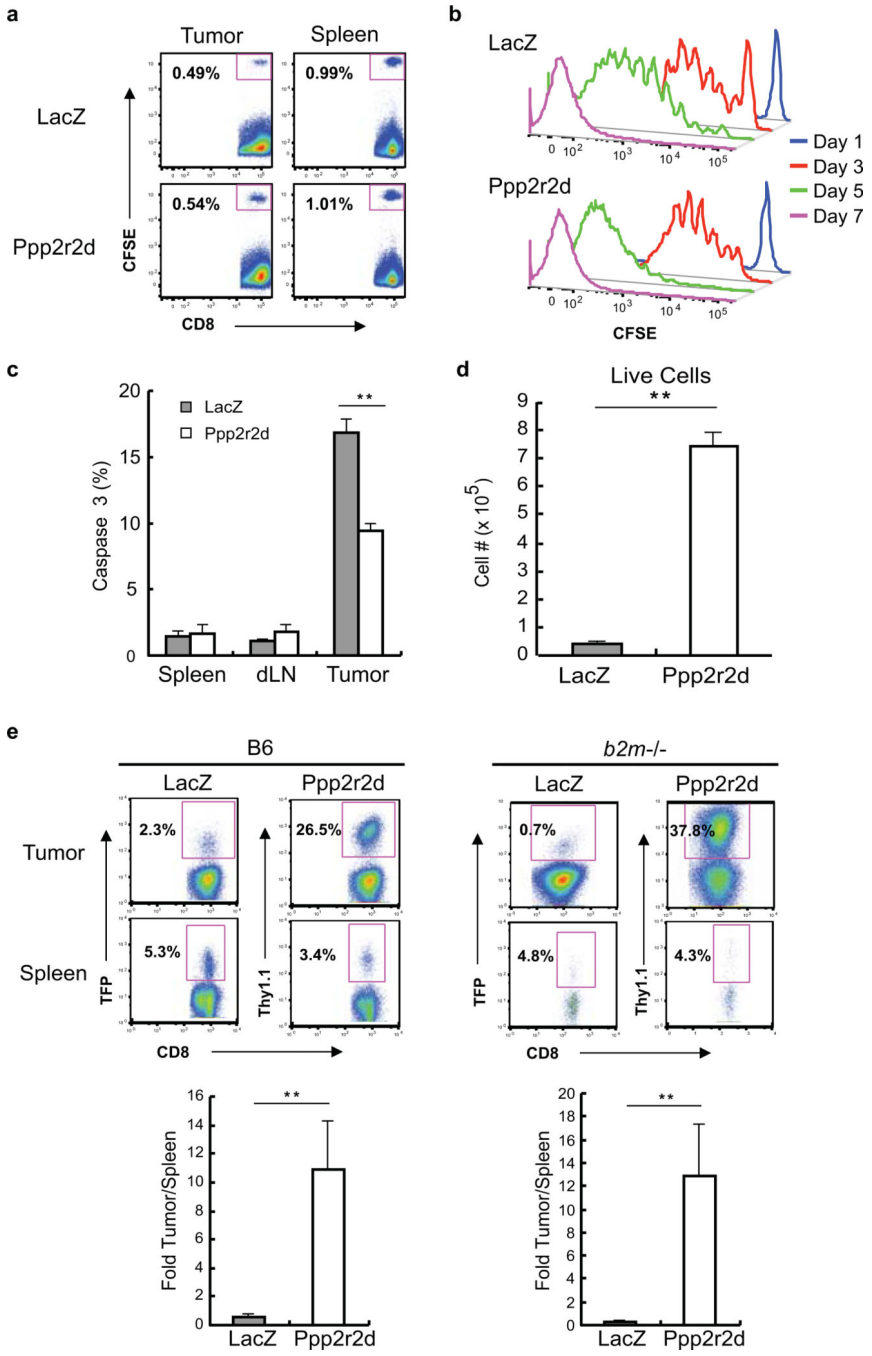

Figure 3. Changes in T cell function induced by Ppp2r2d shRNA

a, Tumor infiltration at 24 hours by CFSE-labeled OT-I T cells. **b**, Enhanced proliferation by Ppp2r2d-silenced T cells (CFSE dilution). **c,d** Reduced apoptosis by Ppp2r2d-silenced OT-I T cell in tumors (**c**, activated caspase-3) or during three day co-culture with B16-Ova tumor cells (**d**, annexin V), **e**, Ppp2r2d-silencing induced T cell expansion even when MHC class I expression was restricted to tumor cells; T cell transfer into C57BL/6 or *b2m*−/− mice with B16-Ova tumors. Data representative of two independent trials (n=3; ** $P<0.01$, two-sided student's *t*-test); mean +/− s.d.

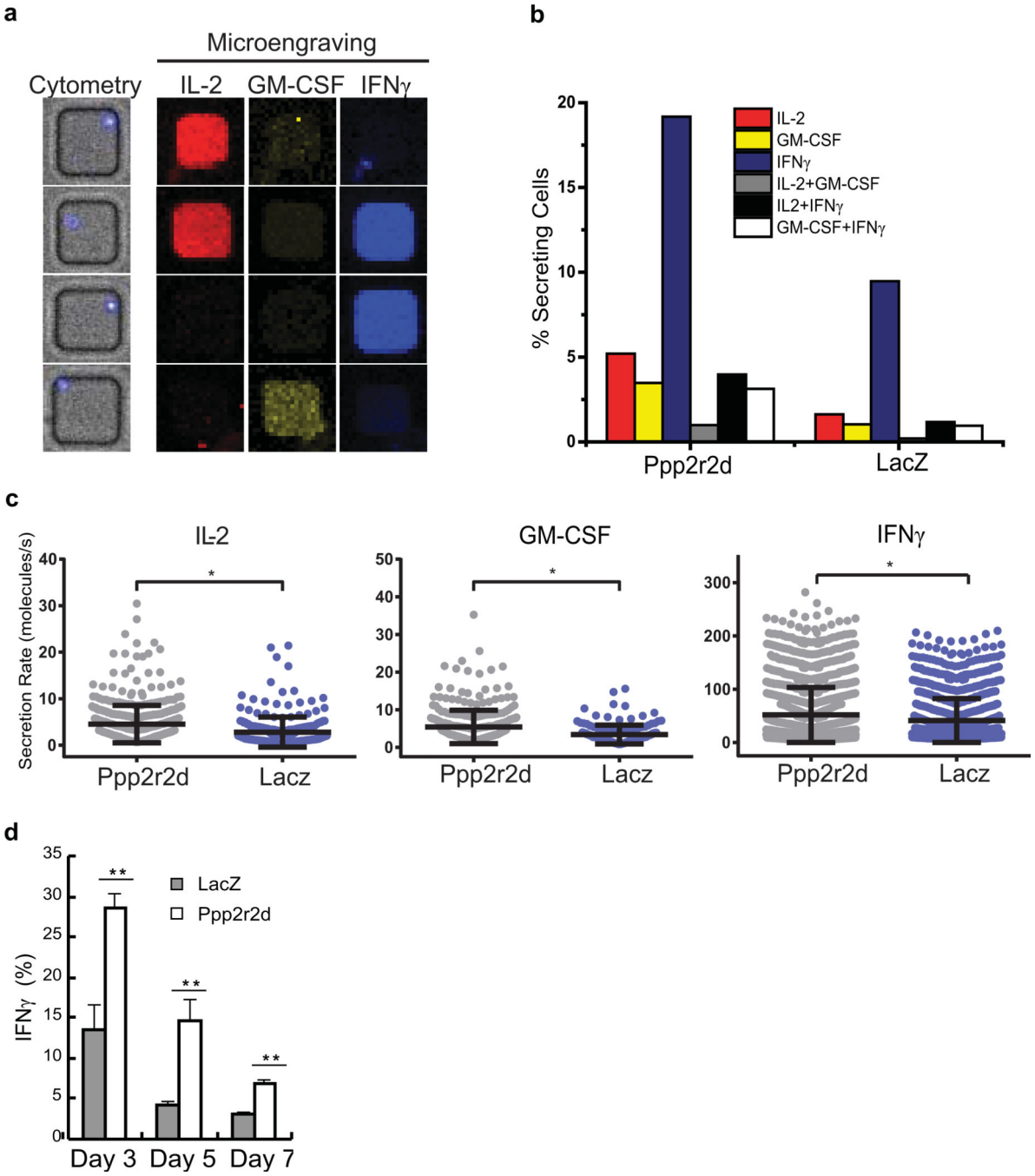

Figure 4. Cytokine secretion by gene-silenced tumor-infiltrating T cells

a–c, *Ex vivo* analysis of cytokine production by tumor-infiltrating OT-I T cells at a single-cell level using a nanowell device (84,672 wells of picoliter volume). **a,** Representative single cells in nanowells and corresponding patterns of cytokine secretion. **b,** Percentage of T cells secreting indicated cytokines. **c,** Cytokine secretion rates calculated from standard curves (mean +/− s.d., Mann Whitney test * $P<0.05$). **d**, Intracellular IFN-γ staining for tumor-infiltrating Ppp2r2d-silenced T cells, representative of two independent experiments (n=3, ** $P<0.01$, two-sided student's *t*-test); mean +/− s.d.

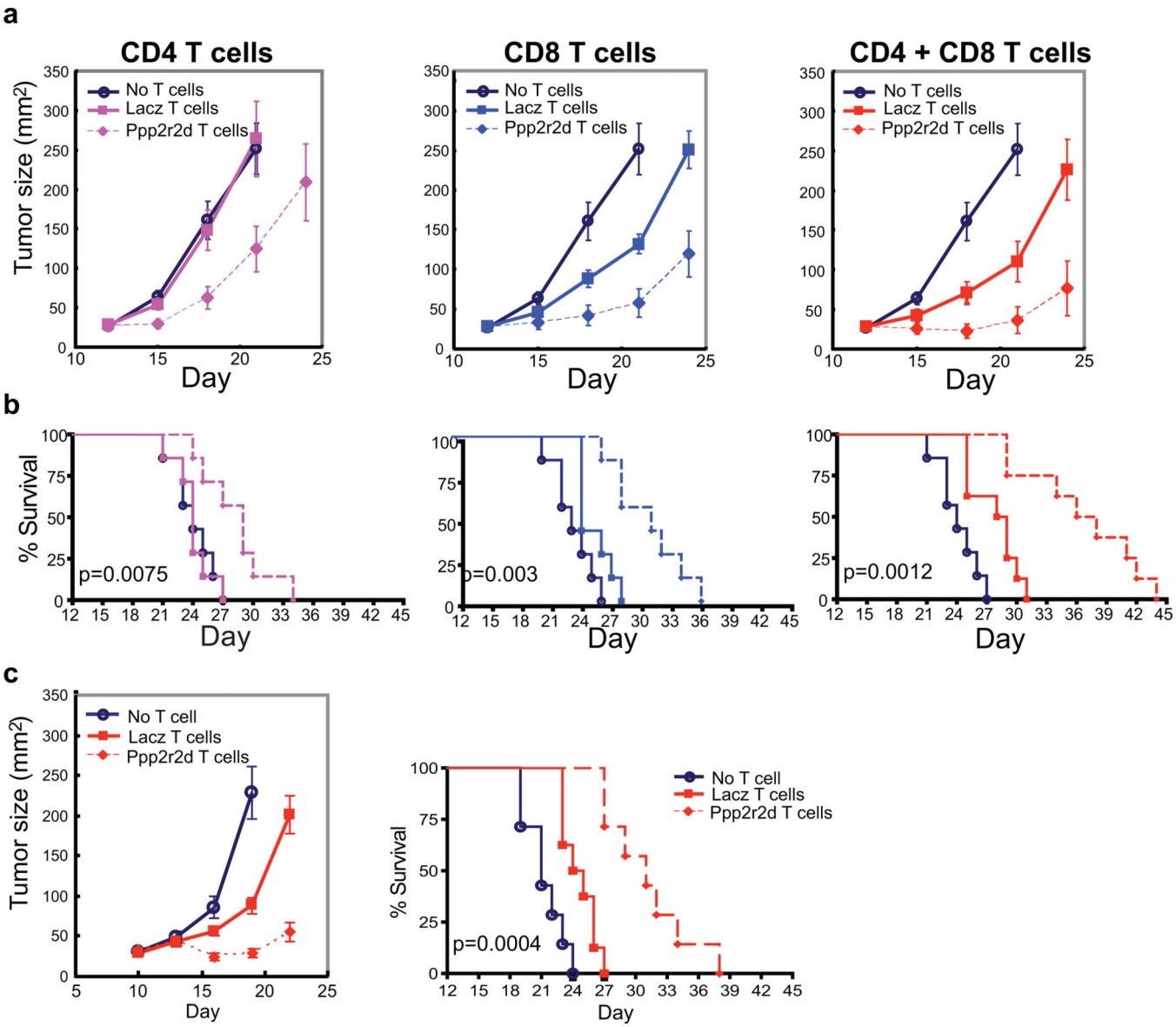

Figure 5. Ppp2r2d silencing enhances anti-tumor activity of CD4 and CD8 T cells

T cells were activated with CD3/CD28 beads and infected with shRNA vectors. **a,b** $CD4^+$ TRP-1 and/or $CD8^+$ OT-I T cells (2×10^6) were transferred (day 12 and 17) into mice bearing day 12 B16-Ova tumors. Tumor burden (**a**) and survival (**b**) were assessed. **c**, $CD4^+$ TRP-1 and $CD8^+$ pmel-1 T cells (3×10^6 each) were transferred (day 10 and 15) into mice with day 10 B16 tumors. Representative of two independent experiments (n=7–9 mice/group), survival analyzed using log-rank (Mantel-Cox) test; mean +/− SEM.

Table 1
Summary of primary and secondary shRNA screens

a, T cell dysfunction and kinase/phosphatase screens. Listed are numbers of genes, shRNAs in each gene set and identified candidate genes. Genes were considered positive in secondary screens when ≥3 shRNAs showed ≥4-fold enrichment in tumor relative to spleen. **b**, Functional classification of candidate genes from secondary screens.

a

		T cell Dysfunction	Kinase/ Phosphatase	shRNA Enrichment
1° Screen	Genes	255	1307	4–10×: 123
	shRN As	1275	6535	10–20×: 17
	Candidate Genes	32	82	> 20×: 1
2° Screen	Genes	32	43	4–10×: 191
	shRNAs	480	645	10–20×: 27
	Candidate Genes	17	26	> 20×: 1

b

Function	Genes
Inhibition of TCR signaling	Cblb, Dgka, Dgkz, Fyn, Inpp5b, Ppp3cc, Ptpn2, Stk17b, Tnk1
Phosphoinositol metabolism	Dgka, Dgkz, Impk, Inpp5b, Sbf1
Inhibitory cytokine signaling pathways	Smad2, Socs1, Socs3
AMP signaling, inhibition of mTOR	Entpd1, Prkab2, Nuak
Cell cycle	Cdkn2a, Pkd1, Ppp2r2d
Actin and microtubules	Arhgap5, Mast2, Rock1
Potential nuclear functions	Blvrb, Egr2, Impk, Jun, Ppm1g
Role in cancer cells	Alk, Arhgap5, Eif2ak3, Hipk1, MetN, uak, Pdzk1ip1, Rock1, Yes1